Research Article
doi: 10.1590/01047760202632013690
vol(32), 2026

CERNE

Monitoring soil deformation during a skidding operation using unmanned aerial vehicle derived data

Abdullah E. Akay[1]*, İnanç Taş[1], Teslime Nazilli[1]

[1] Bursa Technical University, Faculty of Forestry, Department of Forestry Engineering, 16310 Bursa, Türkiye.

FOREST MANAGEMENT

ABSTRACT

Background: In recent years, mechanized logging equipment has become more frequently used in topographically suitable and intensively managed forest areas. However, the rut depths caused by this logging equipment can cause serious deformation problems in the forest soil. In this study, the physical impacts of a skidder on forest soil were evaluated using Unmanned Aerial Vehicle (UAV) based digital imagery. The research was conducted in the Saros Forest Enterprise Chief located in the city of Çanakkale in Türkiye, where rut depth formations were comparatively analyzed using manual ruler method and UAV data. Rut depths were determined for two slope classes (0-20% and 20-50%) and during the fifth, tenth, and fifteenth turns of the skidder.

Results: The results indicated that the rut depths calculated from UAV imagery were highly consistent with those obtained from manual measurements. It was observed that rut depths were greater on steeper slopes (20-50%) and increased with the number of turns. In addition, bulk density and hygroscopic moisture tended to increase in low-slope areas while decreasing in steep slopes.

Conclusions: The UAV-based method provides a quick and reliable approach for monitoring soil deformation caused by a skidder during logging operations. This UAV-based method can help predict the environmental impacts of logging equipment and support more sustainable timber extraction planning. Moreover, the proposed methodology can be applied to evaluate the physical effects of other mechanized logging equipment on forest soil.

Keywords: *Forest harvesting;mechanized logging; rut depth; UAV photogrammetry.*

HIGHLIGHTS

UAV imagery accurately measured rut depth caused by skidder operation.
Rut depth increased with both slope steepness and number of skidder passes.
Bulk density and moisture showed contrasting responses depending on slope conditions.
UAV-based monitoring provides a rapid and reliable tool for assessing soil deformation.

AKAY, A. E.; TAŞ, İ.; NAZILLI, T. Monitoring soil deformation during a skidding operation using unmanned aerial vehicle derived data. CERNE, v. 32, e103690, 2026. DOI: 10.1590/01047760202632013690.

✤Corresponding author: abdullah.akay@btu.edu.tr
Scientific Editor: Samuel José Silva Soares da Rocha

Received: January 15 2026
Accepted: May 22 2026

CERNE
ISSN 0104-7760

INTRODUCTION

Mechanized logging equipment used in harvesting operations can cause damage to residual trees and forest soil, particularly when operations are not properly planned from technical and environmental perspectives (Cantar *et al.*, 2022; Lee *et al.*, 2022). Common ecological impacts of these heavy machines include soil disturbance, reduced soil fertility and nutrient content, erosion caused by surface runoff, and degradation of the humus layer (Mohieddinne *et al.*, 2023). The severity of soil damage may vary depending on factors such as machine type, operation intensity, terrain slope, and soil characteristics (Ferencík *et al.*, 2022; Labelle *et al.*, 2022; Parajuli *et al.*, 2022). Among these impacts, soil compaction and rut formation are considered some of the most important problems associated with mechanized skidding operations (Baek *et al.*, 2022; Breinig *et al.*, 2025). Rutting can alter soil properties such as bulk density and moisture content, negatively affecting natural regeneration, root development, site productivity, and soil fauna biodiversity (Kim *et al.*, 2025; Latterini *et al.*, 2024).

Reducing the ecological impacts caused by rut formation is important for sustainable forest operations. Traditionally, rut depth has been measured manually using rulers and laths (Lovrincevic *et al.*, 2024). Although this method is commonly used in field studies, it can be time-consuming and difficult to apply over large or inaccessible areas. GNSS RTK devices have also been used to measure rut depths with centimeter-level accuracy (Luo *et al.*, 2021). However, the performance of these systems may be affected by canopy closure, terrain conditions, and tree species composition (Abdi *et al.*, 2022).

In recent years, UAV photogrammetry has become an important remote sensing technique for obtaining high-resolution three-dimensional data and overcoming some limitations of conventional measurement methods. UAV-based approaches allow faster and more efficient data collection in difficult terrain conditions while covering larger areas (Büyüksakallı *et al.*, 2025).

Previous studies reported strong agreement between UAV-based and manual rut depth measurements, indicating that UAV photogrammetry can reliably monitor soil deformation (Marra *et al.*, 2021; Lovrincevic *et al.*, 2024). In addition, airborne and terrestrial LiDAR technologies have been successfully used to detect soil compaction and rutting under forest canopy conditions (Mohieddinne *et al.*, 2023; Kim *et al.*, 2025). Despite their high accuracy, the operational use of LiDAR systems is still limited by high equipment costs (Hruza *et al.*, 2025). Although UAV photogrammetry has been increasingly used in forestry applications, studies evaluating skidder-induced soil deformation under varying slope and traffic conditions remain limited. Previous UAV-based rutting studies have mainly focused on validating UAV-derived measurements against conventional field methods or on assessing rut formation under specific operational settings. However, studies simultaneously evaluating skidder-induced soil deformation across different slope classes, repeated traffic intensities, and associated soil physical responses remain limited. To address this gap, the present study integrates UAV photogrammetry, manual rut measurements, and soil property observations to evaluate rut development under varying slope and skidder pass conditions. Beyond previous UAV-based studies, this work provides a combined assessment of terrain, traffic intensity, and soil response during active mechanized forest harvesting operations. Therefore, UAV photogrammetry was used to evaluate soil deformation and rut formation caused by a Tigercat 635D skidder. Rut depths obtained from UAV images were compared with manual field measurements, while soil samples collected along skid roads were analyzed to determine changes in bulk density and hygroscopic moisture. Therefore, the main contribution of this study is the integrated evaluation of UAV-derived rut measurements, traffic intensity, slope conditions, and soil response within active mechanized harvesting operations. This study hypothesized that UAV-derived photogrammetric measurements can accurately quantify rut depth and effectively detect soil deformation caused by skidder operations under different slope and traffic conditions.

MATERIAL AND METHODS

Study Area

The study area is compartment number 139 within the boundary of Saros Enterprise Chief (FEC) located in Keşan Forest Enterprise Directorate in the city of Çanakkale in Türkiye (Figure 1). Timber extraction work was carried out in a Brutian pine (*Pinus brutia*) stand with an average slope of 35%. In the study, where the whole tree extraction method was used, the products were skidded from the forest area to the landing with a Tigercat 635D model skidder (Figure 2). The Tigercat 635D skidder used in the study was manufactured in 2016 and had been actively used in forestry operations for approximately six years prior to the field study. Although detailed hour-meter records were not available, the skidder was known to have operated for more than 5,000 hours under standard forestry conditions prior to the field study. During the study period, the machine was in operational condition, and routine maintenance procedures were regularly conducted by the forest enterprise to ensure proper machine performance under standard forestry operating conditions. A DJI Mavic 2 Pro UAV was used to record the skidding operation during field work.

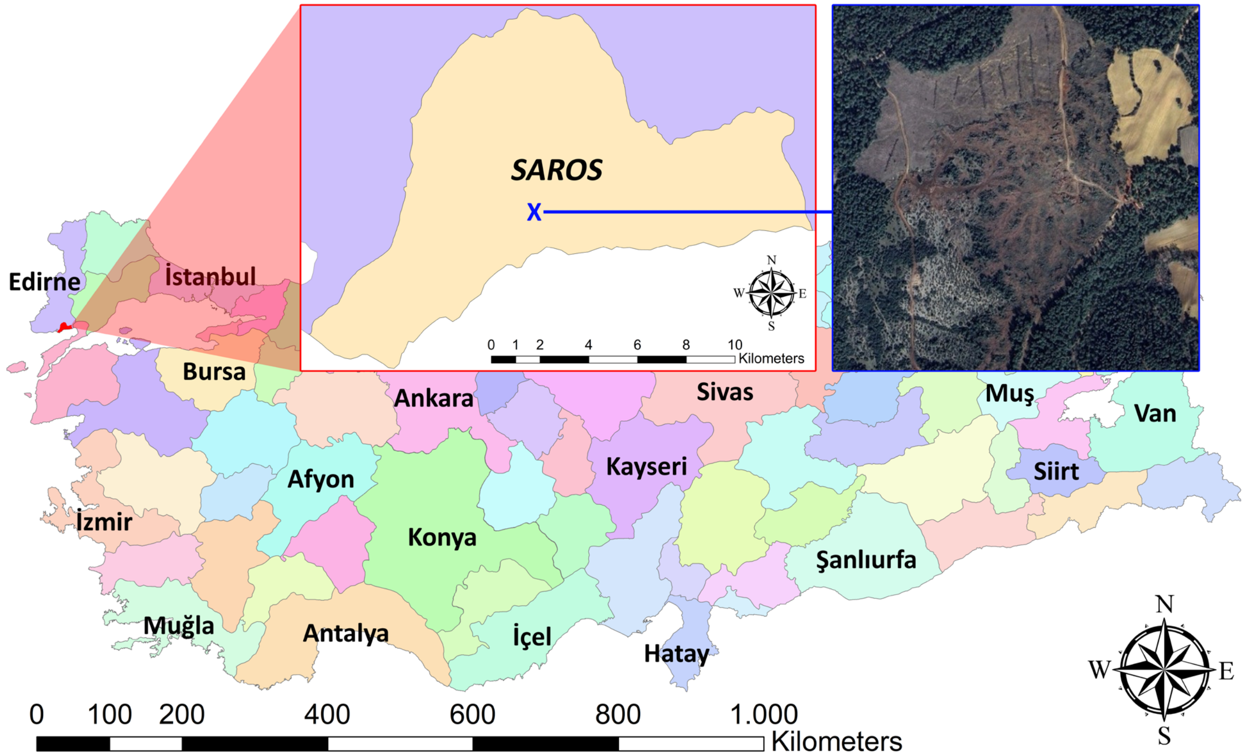

Figure 1: The study area in Saros FEC.

Figure 2: Tigercat 635D model skidder (Photo: İ. Taş).

Soil Impact Measurements

During field studies, measurements were taken regarding the rut depth formed on the ground along the skidding road by the Tigercat 635D model skidder. To examine the possible effect of the slope of the skidding road on the rut depth, the skidding road was divided into two slope groups (0-20% and 20-50%). The slope ranges were determined by taking into account the slope classes defined by IUFRO for primary transportation works in forestry; flat terrain (0-10%), gentle slope (11-20%), moderate slope (21-33%), steep slope (34-50%), and very steep slope (>51%) (Genç and Aricak, 2025). Accordingly, the first slope group (0-20%) falls into the flat terrain and gentle slope category, while the second slope group (20-50%) falls into the moderate and steep slope category. The skidding distance is approximately 60 meters in both slope groups. A 3D model generated from UAV images was used to determine the rut depths formed in the forest soil after the fifth, tenth, and fifteenth turns during skidding. These values were compared with the rut depths measured in three replicates using a ruler and a lath after the fifth, tenth, and fifteenth turns in both slope groups. The original IUFRO slope classes were grouped into two broader categories in order to simplify the field evaluation and ensure sufficient sampling intensity within each operational slope condition.

UAV Data Acquisition

Image acquisition was performed before the start of logging and repeated after the 5th, 10th, and 15th skidder passes. UAV flights were planned using Pix4Dcapture software (Pix4D SA, Lausanne, Switzerland) running on a smartphone connected to the controller. The same flight parameters were applied during each survey in order to keep the datasets comparable. Flights were conducted in Grid Mission mode at an altitude of 50 m, with 80% forward and side overlap, medium flight speed, and a survey area of approximately 131 × 178 m (2.4 ha). Under these settings, a single mission lasted about 11 min. The resulting photographs provided sufficiently uniform coverage for monitoring ground changes associated with skidder traffic.

Photogrammetric Processing and DEM Generation

After the UAV flights, the collected photographs were processed in Agisoft Metashape 1.8.3 (Agisoft LLC, St. Petersburg, Russia). The software was used to organize and align the image sets and to reconstruct the surveyed area from overlapping photographs. Based on this workflow, dense point clouds, elevation data, and orthophoto outputs were produced. The processing procedure made it possible to represent the soil surface in sufficient detail to observe deformation patterns related to skidder movement. Agisoft Metashape was employed because it is commonly used in UAV photogrammetry studies dealing with terrain modeling and surface analysis.

A digital elevation model (DEM) was generated through a series of processing steps. These steps were performed separately for four flights corresponding to the pre-logging, fifth, tenth, and fifteenth turns. The process began with importing the photographs into the program interface and generating tie points (Align Photos). Tie points were then produced on the interface which was followed by verification using six ground control points taken from the study area. To ensure all photos were correctly positioned, the "Optimize Cameras" process was used to align the photos in the same area with the ground control point centers. These corrections reduced positioning and alignment errors associated with UAV acquisition, making the data more accurate and closer to reality. In the next stage after the correction processes, the "Build Dense Cloud" process was used to generate a high-quality dense point cloud by utilizing the connection points. Then, the "Build DEM" process was used to generate a DEM of the study area. The resolution of the DEM obtained using the dense point cloud for four flights was between 2.41-2.49 cm. In the final stage, the Build Orthomosaic process was applied to generate an orthophoto. The resolution of the orthophoto obtained for four flights was between 1.19-1.25 cm. The areas where skidding roads are located on the orthophoto were drawn using the "Draw Polygon" tool to determine the skidding corridor (Figure 3).

Rut Depth Measurements

During the studies, manual measurements were performed using a ruler after the fifth, tenth, and fifteenth turns to measure the rut depths formed by the skidder on the soil. Measurements were made from three sections for

Figure 3: Skidding roads for 0-20% (left) and 20-50% (right) slope groups.

each of the three turns and two slope groups along the skidding roads. The ruler was placed perpendicular to the lath placed at the top of the sections, and the rut depths were read from the ruler. A total of 36 measurements were made (3 turns x 2 slopes x 3 sections x 2 wheels) from two wheel tracks (right and left) in each section for the determined turns (5, 10, and 15) and two slope groups (0-20% and 20-50%). In the next stage, cross-sections were drawn using the Agisoft Metashape 1.8.3 program (Figure 4). Diagrams were generated for these cross-sections using the DEM obtained from the UAV images. The rut depths for both wheels were determined on these cross-sections using the Agisoft Metashape 1.8.3 program.

Statistical Analysis

Statistical analyses were performed using SPSS 20.0 software (IBM Corp., Armonk, NY, USA). Data normality was evaluated using the Shapiro–Wilk test prior to statistical analyses. Differences between UAV-based and ruler measurements were examined using the Paired Sample t-test. In addition, two-way ANOVA was used to evaluate the effects of slope class and skidder pass number on rut depth formation. Before applying ANOVA, normality and homogeneity of variance assumptions were verified using the Shapiro–Wilk and Levene's tests, respectively. The significance level for all analyses was set at $\alpha = 0.05$.

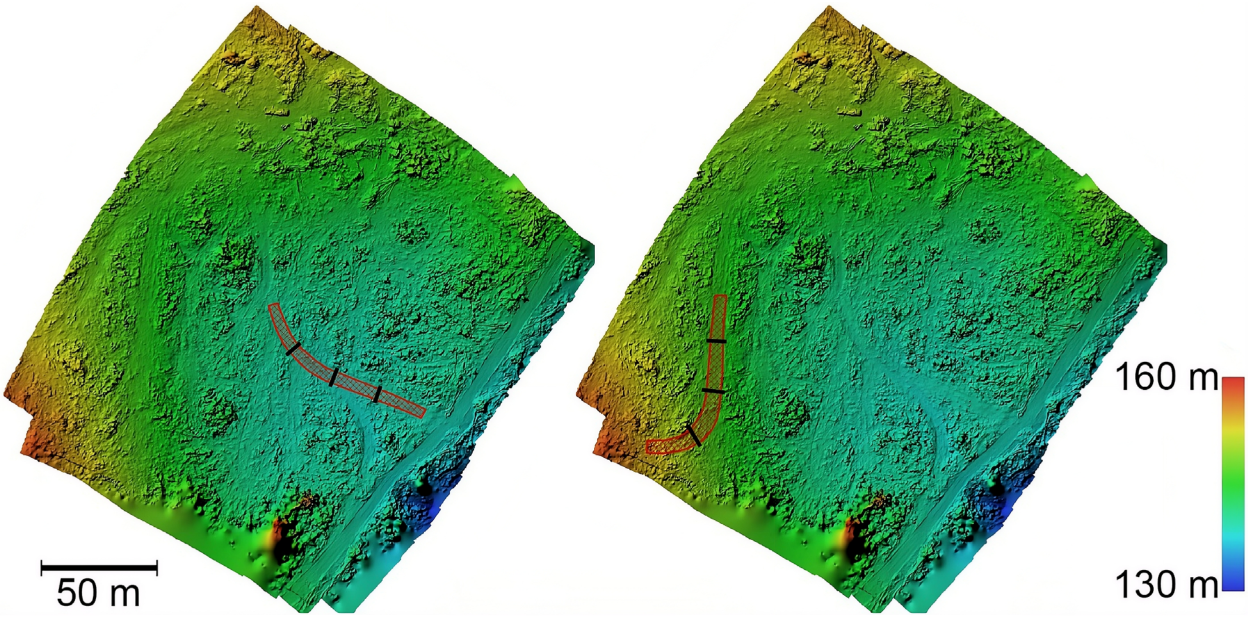

Figure 4: Plan view of three cross-sections along the skidding roads for 0-20% (left) and 20-50% (right) slope groups.

Finally, R^2 and Root Mean Square Error (RMSE) values were calculated to assess agreement between the UAV and manual rut depth measurements.

Soil Analyses

Air-dry weight, oven-dry weight, bulk density, and hygroscopic moisture content of soil samples taken from the study area were determined in the soil laboratories of Bursa Technical University. To investigate the effects of skidding operation on soil properties, soil samples were collected from two slope groups (0-20% and 20-50%) before skidding (control), after the fifth, tenth, and fifteenth turns, and from two soil depth levels (0-5 cm, 5-10 cm). Thus, a total of 16 soil samples were taken: 4 control samples from 2 slope groups and 2 depth levels, and 12 samples from 2 slope groups and 2 depth levels in 3 turns (3 turns x 2 slopes x 2 depths). The reason for choosing two depth levels is that the effects of vehicle movements on the soil are more pronounced, especially in the layers close to the surface. The surface layer (0–5 cm) is the layer most exposed to direct wheel contact, compaction, and sliding effects, and is the region where changes in soil structure and physical properties are first observed. The subsoil (5–10 cm), on the other hand, allows for the evaluation of the distribution of loads transmitted from the surface within the soil profile and the depth-dependent effects of deformation (Hamza and Anderson, 2005). Examining these two depth levels together contributes to a more accurate and comparable understanding of the vertical distribution of the effects of mechanized logging equipment on the soil.

To determine bulk density, soil samples were taken from the study area using iron cylinders (5 cm inner diameter and 5 cm high). In the study area, the cylinder was first driven into the soil at a depth of 0-5 cm and then at depths of 5-10 cm to collect soil samples. These samples were placed in two polyethylene bags with labels indicating the slope class, depth, and sample area. To perform the necessary analyses, the wet soil samples were weighed using a precision balance upon arrival at the laboratory. The soil samples brought from the field were spread on paper in appropriate sections of the laboratories and left to air dry. Following drying, the samples were weighed on precision balances and ground in porcelain mortars. Then, these samples were dried in an oven at 105°C for 24 hours to determine their oven-dry weights (Ferencík *et al.*, 2022). These oven-dry weights were divided by the cylinder volume to calculate the bulk density values (Tavankar *et al.*, 2022). For hygroscopic moisture determination, approximately 10 g of air-dried soil, with a tare weight finer than 2 mm, was placed in a weighing vessel dried at 105°C using the square-cutting method. The soil samples were left in the oven overnight, cooled in a desiccator, and weighed using a precision balance. Soil moisture was calculated as a percentage (%) by finding the difference between these two weightings and dividing this difference by the oven-dried weight (Genç and Aricak, 2025). Due to the limited sample size and lack of replication, soil property results were interpreted descriptively rather than through inferential statistical analysis. The number of soil samples was limited due to operational and logistical constraints during active harvesting operations.

RESULTS

Soil Effect Findings

Using a 3D model produced from UAV images, rut depths formed after the fifth, tenth, and fifteenth skidder passes in the skidding operations conducted in Saros FEC were determined for two slope groups (0–20% and 20–50%). The rut depths were measured using both the manual ruler method and the UAV-based method, and the results obtained from the two methods were compared. According to the comparison conducted using all rut depth data, a strong correlation was found between the rut depth values obtained from the two methods (R^2 = 0.97; $p < 0.001$). RMSE was calculated as 0.896 cm, indicating that the rut depth measurements derived from the UAV-based method achieved an acceptable level of accuracy.

Two-way ANOVA results indicated that both slope class and skidder pass number had significant effects on rut depth formation ($p < 0.001$). Rut depth significantly increased with increasing skidder passes, while steeper slope conditions resulted in greater soil deformation. However, the interaction effect between slope class and skidder pass number was not statistically significant (p = 0.082), indicating that the influence of skidder passes on rut depth was generally similar between slope groups (Table 1).

Table 1: Two-way ANOVA results for rut depth.

Source	df	F	p-value
Slope	1	95.000	<0.001
Pass	2	113.189	<0.001
Slope*Pass	2	2.726	0.082

Fifth Turn

The rut depths obtained using two methods are presented in Table 2 for the fifth turn. According to the UAV data, the average rut depth was 12.17 cm in the 0–20% slope group, compared with 11.23 cm obtained using the ruler method. For the 20–50% slope group, the average rut depth was 15.67 cm for the UAV method and 15.13 cm for the ruler method. A normality test was conducted to evaluate the data distribution. According to the Shapiro–Wilk test, the significance values were greater than 0.05, indicating a normal distribution. Correlation analysis (r = 0.979) indicated a strong positive relationship between the two methods ($p < 0.01$).

Tenth Turn

Table 3 shows the rut depths obtained using two methods for the tenth turn in the study. According to the data obtained with the UAV, the average rut depth was found to be 16.83 cm in the 0-20% slope group, and 16.50 cm for the ruler method. For the 20-50% slope group, the average rut depth was found to be 22.83 cm for the UAV

Table 2: Rut depths (cm) obtained by both methods for the fifth turn.

Slope Group	Sections	Right Wheel (Ruler)	Right Wheel (UAV)	Left Wheel (Ruler)	Left Wheel (UAV)
0–20%	1	10.5	11.0	12.5	13.0
	2	9.5	10.0	12.2	13.0
	3	12.7	14.0	10.0	12.0
20–50%	1	15.5	16.0	13.8	14.0
	2	14.6	15.0	16.2	17.0
	3	16.5	17.0	14.2	15.0

and 22.20 cm for the ruler method. The normality of the data distribution checked by Normality Test confirmed the normal distribution (p>0.05). A correlation analysis was conducted to examine the relationship between the 12 rut depth data obtained using the UAV and ruler method in the tenth turn. The correlation analysis revealed a strong positive relationship (0.984) between the measurement methods ($p < 0.01$).

Fifteenth Turn

The rut depths obtained using two methods were indicated in Table 4 for the fifteenth turn of the study. The average rut depth was found to be 20.67 cm in the 0-20% slope group for the UAV method, and 19.95 cm for the ruler method. For the 20-50% slope group, the average rut depth was found to be 27.00 cm for the UAV and 26.43 cm for the ruler method

According to the Shapiro–Wilk test ($p > 0.05$), the significance values are greater than 0.05, therefore the data conforms to a normal distribution. A correlation analysis was conducted to examine the relationship between the 12 rut depth data obtained using the UAV and ruler method in the fifteenth turn. The correlation analysis results of 0.975 indicated a strong positive correlation between these methods ($p < 0.01$).

For each slope group, rut depth measurements were obtained from three cross-sections during the fifth, tenth, and fifteenth skidder passes. Representative cross-sectional profiles for the slope groups are presented in Figures 5 and 6, respectively. Comparisons of rut depth measurements obtained using the ruler and UAV methods for different slope groups and skidder passes are presented in Figure 7.

Table 3: Rut depths (cm) obtained using both methods for the tenth turn

Slope Class	Sections	Right Wheel (Ruler)	Right Wheel (UAV)	Left Wheel (Ruler)	Left Wheel (UAV)
0–20%	1	15.0	16.0	18.4	18.0
	2	17.5	17.0	14.6	15.0
	3	15.2	16.0	18.3	19.0
20–50%	1	22.4	23.0	20.7	22.0
	2	21.4	21.0	23.2	24.0
	3	21.7	22.0	23.8	25.0

Table 4: Rut depths (cm) obtained using both methods for the fifteenth turn

Slope Class	Sections	Right Wheel (Ruler)	Right Wheel (UAV)	Left Wheel (Ruler)	Left Wheel (UAV)
0–20%	1	17.8	20.0	19.9	21.0
	2	22.0	23.0	20.5	21.0
	3	20.6	21.0	18.9	18.0
20–50%	1	25.9	27.0	23.5	24.0
	2	27.9	29.0	25.8	25.0
	3	29.1	30.0	26.4	27.0

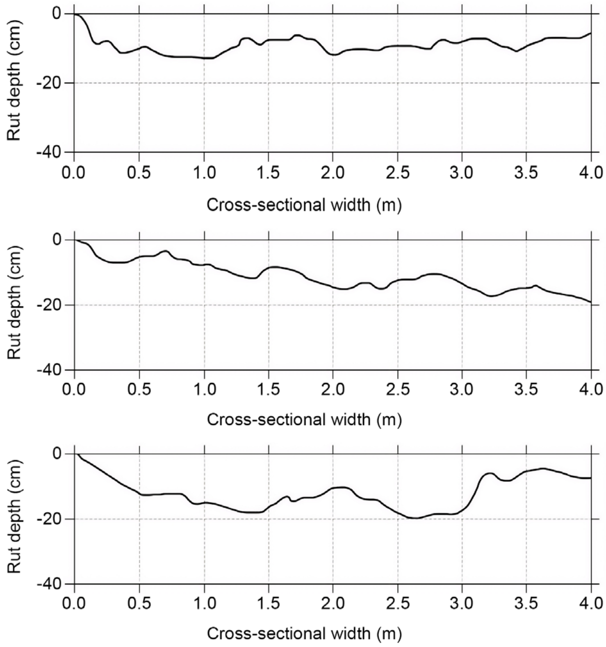

Figure 5: Representative cross-sectional rut profiles derived from UAV-based DEM data after the fifth (a), tenth (b), and fifteenth (c) skidder passes in the 0-20% slope group

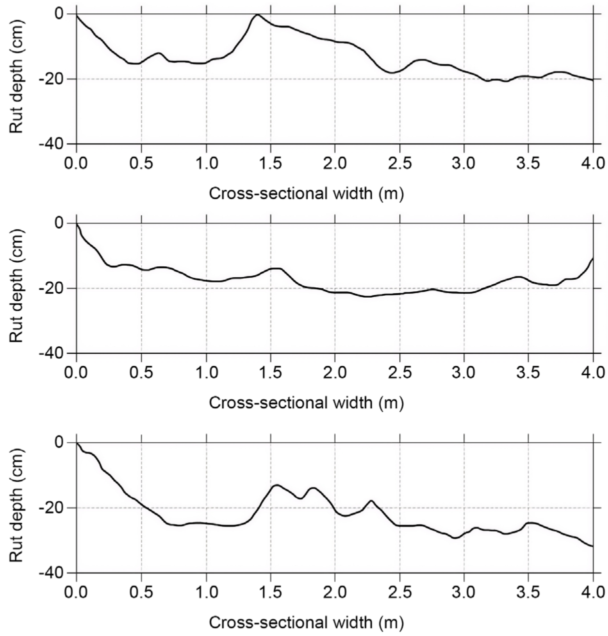

Figure 6: Representative cross-sectional rut profiles derived from UAV-based DEM data after the fifth (a), tenth (b), and fifteenth (c) skidder passes in the 20-50% slope group

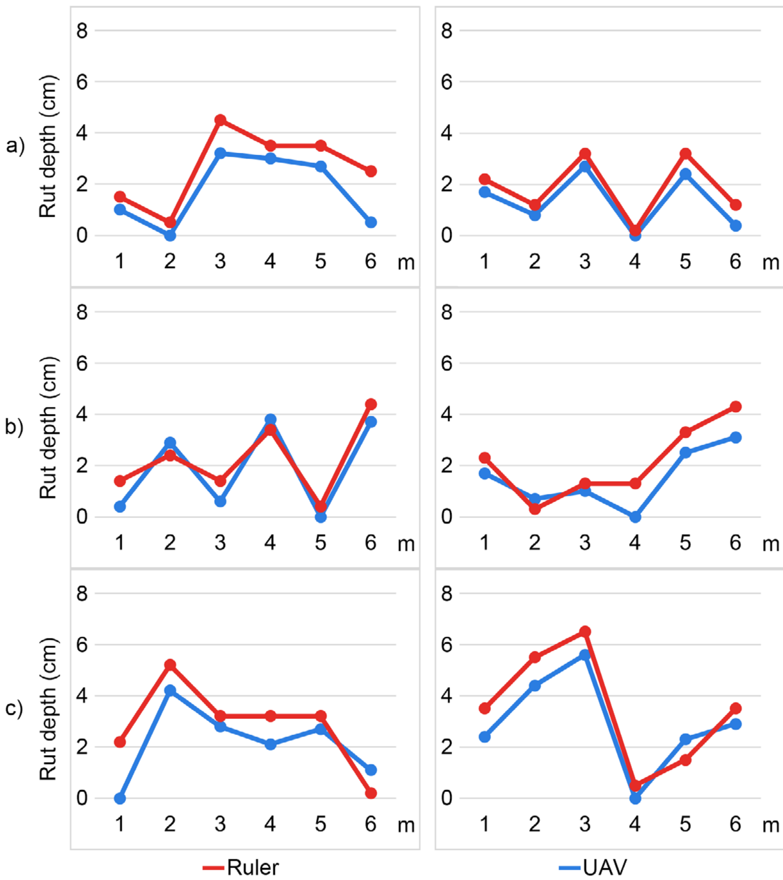

Figure 7: Comparison of rut depth measurements obtained using ruler and UAV methods for the 0–20% and 20–50% slope groups during the (a) fifth, (b) tenth, and (c) fifteenth skidder passes.

Soil Analysis Findings

The average bulk density of the soil samples was determined as 1.08 g/cm3. The highest bulk density (1.77 g/cm3) was found in the control group at a depth of 5-10 cm in the area with a 0-20% slope. The lowest bulk density (0.85 g/cm3) was obtained in the fifteenth turn at a depth of 5-10 cm in 0-20% slope group (Table 5).

According to the hygroscopic moisture analysis results, the average hygroscopic moisture of the soil samples was found to be 2.97%. The lowest hygroscopic moisture (1.94%) was obtained in the tenth turn at a depth of 5-10 cm in the area with a 20-50% slope. The highest hygroscopic moisture content (3.93%) was observed in the 0-5 cm depth in the 0-20% sloped area in the fifteenth turn (Table 6).

Table 5: Results of bulk density analysis of soil samples.

Soil Treatment	Slope (%)	Depth (cm)	Air-Dry Weight (g)	Oven-Dry Weight (g)	Bulk Density (g/cm^3)
Control	0–20	0–5	110.35	107.14	1.09
Control	0–20	5–10	176.87	173.39	1.77
Fifth Turn	0–20	0–5	94.56	91.43	0.93
Fifth Turn	0–20	5–10	107.34	104.87	1.07
Tenth Turn	0–20	0–5	120.64	117.42	1.20
Tenth Turn	0–20	5–10	108.38	104.94	1.07
Fifteenth Turn	0–20	0–5	101.89	98.04	1.00
Fifteenth Turn	0–20	5–10	85.51	82.97	0.85
Control	20–50	0–5	91.66	88.45	0.90
Control	20–50	5–10	100.77	97.15	0.99
Fifth Turn	20–50	0–5	126.70	122.81	1.25
Fifth Turn	20–50	5–10	98.12	95.63	0.98
Tenth Turn	20–50	0–5	121.37	117.80	1.20
Tenth Turn	20–50	5–10	96.92	95.08	0.97
Fifteenth Turn	20–50	0–5	107.38	104.07	1.06
Fifteenth Turn	20–50	5–10	99.89	97.52	1.00

DISCUSSION

Rut depth values obtained from UAV imagery were highly consistent with manual measurements, indicating that UAV photogrammetry can reliably quantify soil deformation caused by skidder operations. The correlation analysis and low RMSE values also supported the reliability of the UAV-based measurements under field conditions. Similar findings were reported by Marra *et al.* (2021) and Lovrincevic *et al.* (2024), who observed strong agreement between UAV-based and conventional rut depth measurements. Compared with traditional field measurements, UAV photogrammetry provides faster data collection, wider spatial coverage, and easier application under difficult terrain conditions.

Rut depth increased with the number of skidder passes in both slope groups, indicating cumulative soil deformation under repeated machine traffic. Repeated skidder passes probably reduced soil resistance and increased rut formation over time. Similar findings were reported by Allman *et al.* (2022), who observed that soil disturbance increased in parallel with the number of machine passes during skidding operations. Differences between slope groups also suggest that terrain conditions affect rut formation through wheel-ground interaction and soil stability. In addition, slope conditions likely influenced rut formation by affecting wheel slip and shear stress during skidding operations (Parajuli *et al.*, 2022). Gülci and Şireli (2019) similarly reported that mechanized logging operations can produce varying rut depths depending on slope conditions and terrain characteristics. Therefore, both

Table 6: Results of hygroscopic moisture analysis of soil samples.

Soil Treatment	Slope (%)	Depth (cm)	Hygroscopic Moisture (%)
Control	0–20	0–5	3.00
Control	0–20	5–10	2.01
Fifth Turn	0–20	0–5	3.42
Fifth Turn	0–20	5–10	2.36
Tenth Turn	0–20	0–5	2.74
Tenth Turn	0–20	5–10	3.28
Fifteenth Turn	0–20	0–5	3.93
Fifteenth Turn	0–20	5–10	3.06
Control	20–50	0–5	3.63
Control	20–50	5–10	3.73
Fifth Turn	20–50	0–5	3.17
Fifth Turn	20–50	5–10	2.60
Tenth Turn	20–50	0–5	3.03
Tenth Turn	20–50	5–10	1.94
Fifteenth Turn	20–50	0–5	3.18
Fifteenth Turn	20–50	5–10	2.43

traffic intensity and slope should be considered during skidding planning to minimize soil disturbance.

In localized sections, relatively greater rut development observed in the 0–20% slope group may be associated with higher soil moisture retention under gentler terrain conditions. Reduced surface runoff in gentler terrain can increase soil softening and decrease soil resistance to wheel pressure, resulting in more pronounced deformation. Previous studies also reported that rut depth tends to increase with increasing soil moisture under forest machine traffic (Labelle *et al*., 2022; Lovrincevic *et al*., 2024). In contrast, steeper slopes generally promote faster drainage and relatively drier soil conditions, which may reduce rut formation despite increased wheel slip. Minor decreases observed in some rut depth measurements may be associated with lateral displacement of loosened soil material from the rut edges during repeated skidder passes.

Soil Analysis

The average bulk density in the control measurements for the 0-20% slope group was found to be 1.43 g/cm^3. The bulk density decreased to 1.00 g/cm^3 in the fifth turn, increased to 1.13 g/cm^3 in the tenth turn, and decreased to 0.92 g/cm^3 in the fifteenth turn. It was found that the bulk density varied with skidder pass number (Marra *et al*., 2022). Mechanized logging operations commonly result in bulk density increases due to soil compaction. While the specific pattern of decreases followed by increases may be influenced by soil moisture, rebound effects or sampling variability, the overall trend of increasing bulk density with repeated vehicle passes is well established (Kim *et al*., 2021). For the 20-50% slope group, the average bulk density in the control group was found to be 0.95 g/cm^3. While the bulk density increased in the fifth turn (1.11 g/cm^3), slight decreases were observed in the tenth (1.09 g/cm^3) and fifteenth (1.03 g/cm^3) turns compared to the fifth turn. In terms of slope groups, bulk density showed increase in skidding operation on the areas exceeding 20% slope. Sohrabi *et al*. (2019) stated that the increase in soil bulk density following logging was greater on slopes exceeding 20% than on slopes below 20% due to slippage of a wheeled skidder.

According to the hygroscopic moisture analysis results for the 0-20% slope group, an increase in hygroscopic moisture content was observed after each turn (fifth turn: 2.89%; tenth turn: 3.01%; fifteenth turn: 3.49%). This increase in hygroscopic moisture can be explained by altered pore size distribution after repeated machine passes (Genç and Aricak, 2025). In the 20-50% slope group, the hygroscopic moisture content decreased in the fifth (2.89%) and tenth turns (2.48%), and increased again in the fifteenth turn (2.81%). Thus, the average hygroscopic moisture content tended to be lower on steeper slopes compared to the 0–20% slope group, likely due to faster gravitational drainage and thinner soil layers on steeper terrain (Cambi *et al*., 2015).

The findings should be evaluated within the context of several study constraints. Soil analyses were derived from a limited number of samples and did not include a replicated sampling framework, which restricts the strength of interpretation regarding bulk density and hygroscopic moisture responses. In addition, observations were obtained from a single operational setting involving one harvesting area and one skidder type. Expanding future investigations to include broader sampling efforts, replicated field designs, and diverse machine–terrain combinations would provide a more robust basis for extending these results to other forestry conditions.

CONCLUSIONS

The results showed that UAV photogrammetry can be successfully used to measure rut depth and monitor soil deformation caused by skidder operations on different slopes. The UAV measurements were generally consistent with the manual field measurements, suggesting that the method provides acceptable accuracy for forestry applications. In addition, UAV surveys made data collection faster and easier, especially in steep and hard-to-access areas. The proposed method also offers a simpler and lower-cost alternative compared with LiDAR-based systems for evaluating soil disturbance.

The results indicated that rut depth usually increased after repeated skidder passes, although the level of disturbance changed depending on slope conditions. This shows that both traffic frequency and terrain structure affect the degree of soil deformation. Changes observed in bulk density and hygroscopic moisture also revealed that mechanized skidding can influence soil properties. Considering these findings, UAV-based monitoring may help forest managers better evaluate soil impacts and improve the planning of harvesting operations to reduce environmental disturbance.

AUTHORSHIP CONTRIBUTION

Project Idea: AEA; İT; TN;
Funding: AEA., İT
Database: İT; TN;
Processing: AEA; İT; TN;
Analysis: AEA; İT; TN;
Writing: AEA; İT; TN;
Review: AEA; İT; TN.

DATA AVAILABILITY:

The datasets supporting the conclusions are included in the article.

REFERENCES

ABDI, O.; UUSITALO, J.; PIETARINEN, J.; *et al.* Evaluation of forest features determining GNSS positioning accuracy of a novel low-cost, mobile RTK system using LiDAR and TreeNet. Remote Sensing, v. 14, p. 2856, 2022. DOI: 10.3390/rs14122856.

ALLMAN, M.; DUDÁKOVÁ, Z.; JANKOVSKÝ, M.; *et al.* Soil compaction after increasing the number of wheeled tractors passes on forest soils in west Carpathians. Forests, v. 13, p. 109, 2022. DOI: 10.3390/f13010109.

BAEK, K.; LEE, E.; CHOI, H.; *et al.* Impact on soil physical properties related to a high mechanization level in the row thinning of a Korean pine stand. Land, v. 11, n. 3, p. 329, 2022. DOI: 10.3390/land11030329.

BREINIG, L.; HINTE, B.; SCHÖNAUER, M.; *et al.* Traction assistance of a forwarder in flat terrain: effects on wheel slip and soil disturbance. Croatian Journal of Forest Engineering, v. 46, n. 1, 2025. DOI: 10.5552/crojfe.2025.2434.

BÜYÜKSAKALLI, H.; TAŞ, İ.; AKAY, A. E. Assessing rut depth formation in a skidding operation using UAV photogrammetry. European Journal of Forest Engineering, v. 11, n. 2, p. 184–191, 2025. DOI: 10.33904/ejfe.1751349.

CAMBI, M.; CERTINI, G.; NERI, F.; *et al.* The impact of heavy traffic on forest soils: A review. Forest Ecology and Management, v. 338, p. 124–138, 2015. DOI: 10.1016/j.foreco.2014.11.022.

CANTAR, I. C.; CIONTU, C. I.; DINCA, L.; *et al.* Damage and tolerability thresholds for remaining trees after timber harvesting: a case study from Southwest Romania. Diversity, v. 14, n. 3, p. 193, 2022. DOI: 10.3390/d14030193.

FERENCÍK, M.; DUDÁKOVÁ, Z.; KARDOS, M.; *et al.* Measuring soil surface changes after traffic of various wheeled skidders with close-range photogrammetry. Forests, v. 13, n. 7, p. 976, 2022. DOI: 10.3390/f13070976.

GENÇ, Ç. Ö.; ARICAK, B. Impact of forestry operations on forest soil respiration depending on stands features in Kastamonu, Türkiye. CERNE, v. 31, p. e103423, 2025. DOI: 10.1590/01047760202531013423.

GÜLCI, S.; ŞIRELI, S. The evaluation of SfM technique in the determination of surface deformation on skidding roads following timber harvesting. European Journal of Forest Engineering, v. 5, n. 2, p. 52–60, 2019. DOI: 10.33904/ejfe.600860.

HAMZA, M. A.; ANDERSON, W. K. Soil compaction in cropping systems: A review of the nature, causes and possible solutions. Soil and Tillage Research, v. 82, n. 2, p. 121–145, 2005. DOI: 10.1016/j.still.2004.08.009.

HRUZA, P.; MIKITA, T.; ZIZLAVSKA, N. Application of unmanned aerial vehicle and airborne light detection and ranging technologies to identifying terrain obstacles and designing access solutions for the interior parts of forest stands. Forests, v. 16, n. 5, p. 729, 2025. DOI: 10.3390/f16050729.

KIM, I.; HAN, S. K.; ACUNA, M.; *et al.* Effect of heavy machine traffic on soil CO2 concentration and efflux in a Pinus koraiensis thinning stand. Forests, v. 12, n. 11, p. 1497, 2021. DOI: 10.3390/f12111497.

KIM, I.; SEO, J.; WOO, H.; *et al.* Assessing rutting and soil compaction caused by wood extraction using traditional and remote sensing methods. Forests, v. 16, n. 1, p. 86, 2025. DOI: 10.3390/f16010086.

LABELLE, E. R.; HANSSON, L.; HÖGBOM, L.; *et al.* Strategies to mitigate the effects of soil physical disturbances caused by forest machinery: A comprehensive review. Current Forestry Reports, v. 8, p. 20–37, 2022. DOI: 10.1007/s40725-021-00155-6.

LATTERINI, F.; SPINELLI, R.; VENANZI, R.; *et al.* Acorn review: focus on ground-based extraction systems: is skidding really more impactful than forwarding? Forest Ecology and Management, v. 551, p. 121514, 2024. DOI: 10.1016/j.foreco.2023.121514.

LEE, E.; EU, S.; LI, Q. Assessment of soil erosion potential from the disturbed surface of skid trails in small shovel harvesting system. Frontiers in Environmental Science, v. 10, p. 756848, 2022. DOI: 10.3389/fenvs.2022.756848.

LOVRINCEVIC, M.; PAPA, I.; POPOVIC, M.; *et al.* Methods of rut depth measurements on forwarder trails in lowland forest. Forests, v. 15, n. 6, p. 1021, 2024. DOI: 10.3390/f15061021.

LUO, X.; SCHAUFLER, S.; BRANZANTI, M.; *et al.* Assessing the benefits of Galileo to high-precision GNSS positioning–RTK, PPP and post-processing. Advances in Space Research, v. 68, n. 12, p. 4916–4931, 2021. DOI: 10.1016/j.asr.2020.08.022.

MARRA, E.; LASCHI, A.; FABIANO, F.; *et al.* Impacts of wood extraction on soil: assessing rutting and soil compaction caused by skidding and forwarding by means of traditional and innovative methods. European Journal of Forest Research, v. 141, p. 71–86, 2022. DOI: 10.1007/s10342-021-01420-w.

MARRA, E.; WICTORSSON, R.; BOHLIN, J.; *et al.* Remote measuring of the depth of wheel ruts in forest terrain using a drone. International Journal of Forest Engineering, v. 32, n. 3, p. 224–234, 2021. DOI: 10.1080/14942119.2021.1916228.

MOHIEDDINNE, H.; BRASSEUR, B.; GALLET-MORON, E.; *et al*. Assessment of soil compaction and rutting in managed forests through an airborne LiDAR technique. Land Degradation and Development, v. 34, n. 5, p. 1558–1569, 2023. DOI: 10.1002/ldr.4553.

PARAJULI, M.; HIESL, P.; HAGAN, D.; *et al*. Logging operations and soil compaction. Clemson: Land-Grant Press, 2022.

SOHRABI, H.; JOURGHOLAMI, M.; TAVANKAR, F.; *et al*. Post-harvest evaluation of soil physical properties and natural regeneration growth in steep-slope terrains. Forests, v. 10, n. 11, p. 1034, 2019. DOI: 10.3390/f10111034.

TAVANKAR, F.; NIKOOY, M.; EZZATI, S.; *et al*. Long-term assessment of soil physicochemical properties and seedlings establishment after skidding operations in mountainous mixed hardwoods. European Journal of Forest Research, v. 141, p. 571–585, 2022.